Site-Specific DNA Transesterification by Vaccinia Topoisomerase: Role of Specific Phosphates and Nucleosides†

Chonghui Cheng and Stewart Shuman*

Molecular Biology Program, Sloan-Kettering Institute, New York, New York 10021

Received August 26, 1999; Revised Manuscript Received October 13, 1999

ABSTRACT: Vaccinia topoisomerase forms a covalent DNA-(3′-phosphotyrosyl)-enzyme intermediate at a pentapyrimidine target site 5′-CCCTTp↓ in duplex DNA. Here we present experiments that illuminate the contributions of specific nucleosides and phosphates to site affinity and transesterification. We find that the −1 phosphate and −2 nucleoside on the scissile strand (5′-CCCTTp↓N**pN**) enhance the rate of transesterification by factors of 40 and 25, respectively, whereas the DNA segment downstream of the −2 nucleotide makes no significant kinetic contribution. Placement of a 5′-phosphate/3′-OH nick at position +2, +3, +4, or +5 within the CCCTT element results in a 5−10-fold reduction in the affinity of topoisomerase binding to DNA. A nick at the +2 phosphate also slows the rate of transesterification by ∼500-fold. This finding, together with earlier studies of the effects of position-specific base and sugar modifications, points to the +2 Tp nucleotide as being the most critical element of the CCCTT target site other than the scissile phosphate itself. On the noncleaved strand, the segment downstream of the 3′-GGGAA element contributes minimally to the rate of transesterification provided that the substrate is otherwise fully base-paired within the 5′-CCCTT target site. By studying the effects of single nucleotide gaps and missing phosphate nicks within the 3′-GGGAA sequence, we find that the +1 and +2 adenosine nucleosides enhance the rate of transesterification by 20- and 1000-fold respectively and that the +5 phosphate (3′-G**p**GGAA) is also important for cleavage. Cumulative functional analyses of the vaccinia topoisomerase−DNA interface are discussed in light of newly available structures for the vaccinia and human type IB enzymes.

Vaccinia topoisomerase, a eukaryotic type IB enzyme, cleaves and reseals DNA through a covalent DNA-(3′-phosphotyrosyl)-enzyme intermediate (*1*). The vaccinia topoisomerase is distinguished from the nuclear type IB enzymes by its stringent site specificity in covalent adduct formation on duplex DNA. Its target site is a pentapyrimidine sequence 5′ (C/T)CCTTp↓ (*2*). The catalytic cycle of vaccinia topoisomerase has been deconstructed into a series of partial reactions: (i) noncovalent binding of enzyme to duplex DNA (*2*−*4*); (ii) nucleophilic attack of Tyr-274 on the Tp↓N phosphodiester of the CCCTTp↓N strand, resulting in formation of a covalent enzyme−DNA intermediate and a noncovalently held 5′ OH strand (*5*, *6*); (iii) free rotation of the noncovalently held downstream duplex around the phosphodiester bond opposite the nick (*7*); (iv) religation via attack of the 5′ OH strand on the 3′ phosphotyrosyl linkage (*6*, *8*−*10*); and (v) dissociation of the enzyme from the DNA (*11*).

The chemistry of DNA transesterification by vaccinia topoisomerase has been dissected using synthetic model substrates containing a single CCCTT site. Comprehensive mutational analysis of the enzyme has led to the identification of the catalytic amino acid residues and, via kinetic analysis, to a quantitative appreciation of their contributions to the topoisomerase-mediated enhancement of the rate of transesterification (*12*−*16*). Our present view is that the major factor in the enzymatic rate enhancement is the stabilization of the presumptive pentacoordinate phosphorane transition state by a network of interactions between the scissile phosphate and specific arginine and histidine side chains of the enzyme (*1*).

The molecular interactions on the DNA side that contribute to target site recognition and catalysis have also been examined using synthetic substrates, but the analysis to date has been largely qualitative. The dimensions of the topoisomerase−DNA interface have been probed by various footprinting methods. The DNase I footprint of bound topoisomerase covers ∼13 nucleotides upstream (5′) and ∼9−13 nucleotides downstream (3′) of the scissile bond (*3*). Modification interference, modification protection, analogue substitution, and UV cross-linking experiments indicate that vaccinia topoisomerase makes contact with several nucleotide bases and the sugar−phosphate backbone of DNA in the vicinity of the CCCTT recognition site (*3*, *17*−*19*). For example, dimethyl sulfate protection and interference experiments revealed interactions with the three guanine bases of the pentamer motif complementary strand (3′-**GGG**AA) (*17*).

The contributions of individual phosphates to binding specificity were inferred from the effects of phosphate ethylation on protein binding (*18*). Ethylation of four phosphates on the scissile strand (positions C**p**C**p**T**p**T**p**↓ within the pentamer motif) and three phosphates on the nonscissile strand (3′-G**p**G**p**G**p**A) interfered with topoisomerase−DNA

† Supported by NIH Grant GM46330.

* To whom correspondence should be addressed. Phone: (212) 639-7145. Fax: (212) 717-3623. E-mail: s-shuman@ski.mskcc.org.

10.1021/bi992001d CCC: $18.00
Published on Web 11/17/1999

complex formation. In a B-form structure of the CCCTT-containing DNA substrate, the relevant topoisomerase−phosphate contacts are arrayed across the minor groove of the DNA helix (*18*). The major groove base-specific contacts that comprise the topoisomerase−DNA interface are situated on the opposite face of the DNA helix from the specific phosphate contacts and from the scissile phosphate. These results suggested that topoisomerase binds circumferentially to its target site in duplex DNA (*18*).

Subsequent structural analyses of the vaccinia and human topoisomerases revealed that the type IB enzymes do indeed form a C-shaped protein clamp around the DNA duplex (*20*−*22*). In both cases, it is the carboxyl-terminal domain containing the catalytically essential side chains that interacts with the minor groove face of the DNA at the cleavage site, while the N-terminal domain is positioned on the major groove side of the target site. The crystal structures and predicted structural models for human and vaccinia topoisomerases, together with functional studies of the vaccinia enzyme (*23*−*25*), imply that significant conformational changes in the enzyme (and probably the DNA as well) are part and parcel of the topoisomerase catalytic cycle (*22*).

In the present study, we examine the DNA component of the topoisomerase−DNA interface. First, we use exonuclease III to obtain a finer map of the size of the topoisomerase-binding site on DNA. The results indicate that the enzyme interacts tightly with the DNA within the CCCTT motif and less tightly with upstream flanking DNA. Second, we address the functional contributions of individual phosphates and nucleosides within and immediately 3′ of the CCCTT target site. We identify kinetically significant roles for the +2 phosphate, the −2 nucleoside, and the −2 phosphate of the scissile strand (5′-CCCT**p**Tp↓N**pN**) in transesterification chemistry, as well as important roles for the +5 phosphate and +1A and +2A nucleosides (3′-G**p**GG**AA**) of the nonscissile strand.

EXPERIMENTAL PROCEDURES

Enzyme Purification. Vaccinia topoisomerase was expressed in *Escherichia coli* BL21 cells infected with bacteriophage λCE6 and then purified from a soluble bacterial lysate by phosphocellulose column chromatography (*26*). The protein concentration of the phosphocellulose preparation was determined by using the dye-binding method (Bio-Rad) with bovine serum albumin as the standard.

Preparation of Radiolabeled DNA Substrates. DNA oligonucleotides were 5′ end-labeled by enzymatic phosphorylation in the presence of [γ^{32}P]ATP and T4 polynucleotide kinase, then purified by preparative electrophoresis through a 17% polyacrylamide gel containing TBE (90 mM Tris-borate and 2.5 mM EDTA). The labeled oligonucleotides were eluted from an excised gel slice and then hybridized to unlabeled complementary oligonucleotide(s) as specified in the figure legends. Annealing reaction mixtures containing 0.2 M NaCl and oligonucleotides as specified were heated to 70 °C and then slow-cooled to 22 °C. The hybridized DNAs were stored at 4 °C.

RESULTS

Exonuclease III Footprint of Vaccinia Topoisomerase on the Noncleaved Strand of CCCTT-Containing Duplex DNA. Previous studies revealed that vaccinia topoisomerase protects the region around the site of covalent adduct formation from digestion with DNase I (*3*). This technique afforded only a rough estimate of the size of the protein−DNA interface, because DNase I did not cleave most of internucleotide bonds in the vicinity of the CCCTT target site. To fine map the margins of the topoisomerase-binding site on DNA, we subjected the topoisomerase−DNA complex to footprinting with exonuclease III, which digests DNA from the 3′ end in single nucleotide increments.

The dimensions of the protected region upstream of the cleavage site were determined by reacting topoisomerase with a CCCTT-containing ligand radiolabeled with ^{32}P at the 5′ end of the 60-mer nonscissile DNA strand (Figure 1A). The substrate includes a 30 bp duplex segment upstream of the scissile phosphate and a short duplex segment downstream. Covalent adduct formation at the CCCTT target site of the 36-mer scissile strand is near-quantitative (>90% of input DNA cleaved) when topoisomerase is added in 5-fold molar excess over DNA (data not shown). The transesterification reaction proceeds to completion because the 6-mer leaving strand 5′ ATTCCC diffuses away from the covalent complex. Topoisomerase−DNA mixtures and a control sample containing DNA alone were treated with exonuclease III. The 5′-labeled digestion products were resolved by denaturing gel electrophoresis and detected by autoradiography. The amount of exonuclease III included in the reactions was sufficient to convert nearly all of the input ^{32}P-labeled 60-mer into rapidly migrating species of ≤22 nucleotides during a 2 min incubation at 22 °C (Figure 1A). Binding of topoisomerase to the DNA resulted in the appearance of two nuclease-resistant clusters at the expense of the shorter digestion products. A prominent doublet of 43 and 44 nucleotides was observed after 2 min of nuclease digestion, along with a shorter doublet of 39 and 38 nucleotides. The longer doublet decayed after 5 min as the 39/38 doublet increased. In turn, the 39-mer declined at 10 and 15 min as the 38-mer species became predominant and a minor 37-mer appeared. We surmise from these results that (i) the covalently bound topoisomerase interacts tightly with a ∼7−9 nucleotide segment of the nonscissile strand immediately upstream of the site of covalent attachment and (ii) the enzyme interacts loosely with the nonscissile strand over the region extending proximally to about positions +13 to +14.

The extent of the inner footprint on the nonscissile strand was examined in greater detail using a different single-turnover cleavage substrate containing 12 bp of DNA upstream of the scissile phosphate and an 18-nucleotide single-strand tail on the nonscissile strand of the covalent complex (Figure 1B). Because the 12-nucleotide duplex is shorter than the outer margins of the exonuclease III footprint observed in Figure 1A, we expected to detect only the inner margin of exonuclease III protection. When the DNA substrate alone was treated with exonuclease III, the 5′-labeled 30-mer nonscissile strand was converted quantitatively into shorter chains of 10−18 nucleotides. Preincubation of the DNA with topoisomerase resulted in the appearance of 27- and 28-nucleotide products after 2 min of nuclease treatment. These species were converted into a doublet of 26-mer and 27-mer strands that was protected completely from further digestion during a 15 min incubation (Figure

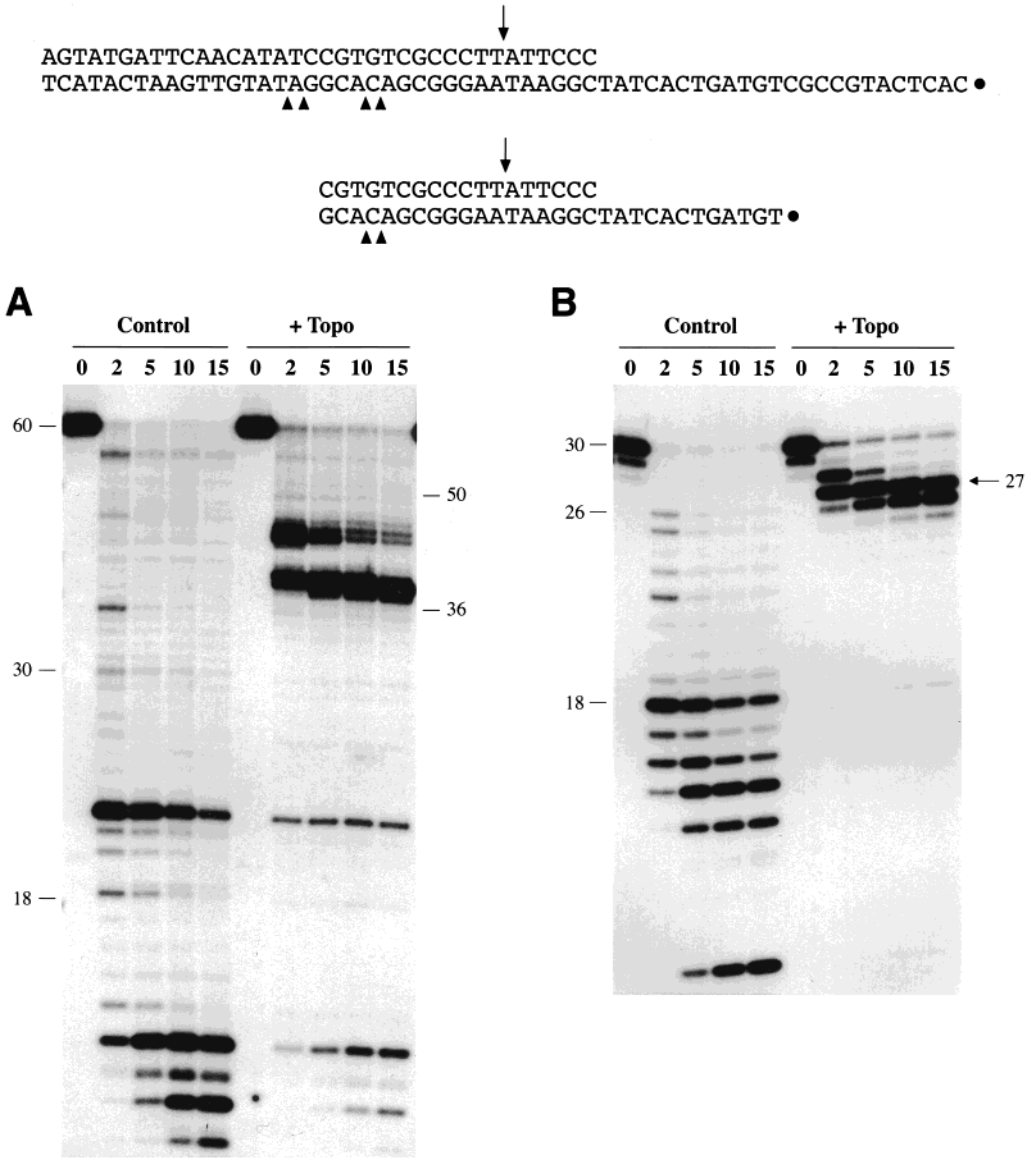

FIGURE 1: Exonuclease III footprint of vaccinia topoisomerase on the noncleaved strand of CCCTT-containing duplex DNA. The structures of the CCCTT-containing substrates are shown. The site of covalent adduct formation is indicated by a vertical arrow. The 5′ ^{32}P-label on the noncleaved strand is denoted by a dot. The margins of the exonuclease III footprints on the nonscissile strand are marked by arrowheads. Reaction mixtures (60 μL) containing 50 mM Tris HCl (pH 7.5), 1 mM $MgCl_2$, 3 pmol of DNA substrate (36-mer/60-mer in panel A or 18-mer/30-mer in panel B), and 15 pmol of topoisomerase were incubated for 15 min at 22 °C. Control reaction mixtures lacking topoisomerase were incubated in parallel. Footprinting reactions were initiated by the addition of exonuclease III (25 units; purchased from New England Biolabs) to the mixtures. Aliquots (10 μL) withdrawn after incubation for 2, 5, 10, and 15 min at 22 °C were quenched immediately by the addition of 1 μL of 0.5 M EDTA and 10 μL of formamide. The time 0 samples were taken prior to the addition of exonuclease III. The samples were analyzed by electrophoresis through a 17% polyacrylamide gel containing 7 M urea in TBE buffer. Autoradiographs of the gels are shown. The positions and sizes of coelectrophoresed 5′-labeled DNA oligonucleotide markers are indicated.

1B). This experiment reveals a clearly demarcated margin of the topoisomerase footprint eight to nine nucleotides upstream of the cleavage site.

Exonuclease III Footprint of Vaccinia Topoisomerase on the Cleaved Strand of CCCTT-Containing Duplex DNA. Interaction of vaccinia topoisomerase with the DNA downstream of CCCTT site was examined using a 60-bp substrate uniquely labeled at the 5′ end of the scissile strand. The topoisomerase binds to the CCCTT target site and establishes a cleavage-religation equilibrium ($K_{cl} \approx 0.25$) that favors the noncovalently bound state. Treatment of the topoisomerase-([^{32}P]DNA) mixture with exonuclease III probes only the DNA interface of the noncovalently bound topoisomerase. Covalent adduct formation results in transfer of the incised 5′-labeled 30-mer to Tyr-274 of the enzyme, thus rendering the 30-mer resistant to exonuclease III digestion. Moreover, the covalent protein−DNA complex does not migrate into the gel during electrophoresis; instead, its formation is detected by the presence of a radiolabeled species that remains in the sample well (not shown).

As shown in Figure 2, the DNA substrate alone is converted by exonuclease III into 5′-labeled fragments of $\leq$12 nucleotides. Exonuclease III treatment of the topoisomerase−DNA complex results in the transient appearance of a protected 41-mer/42-mer doublet after 2 min of digestion; the doublet disappears at later times, and there is scant accumulation of shorter digestion products. Instead, the label is transferred to the well (not shown). This indicates

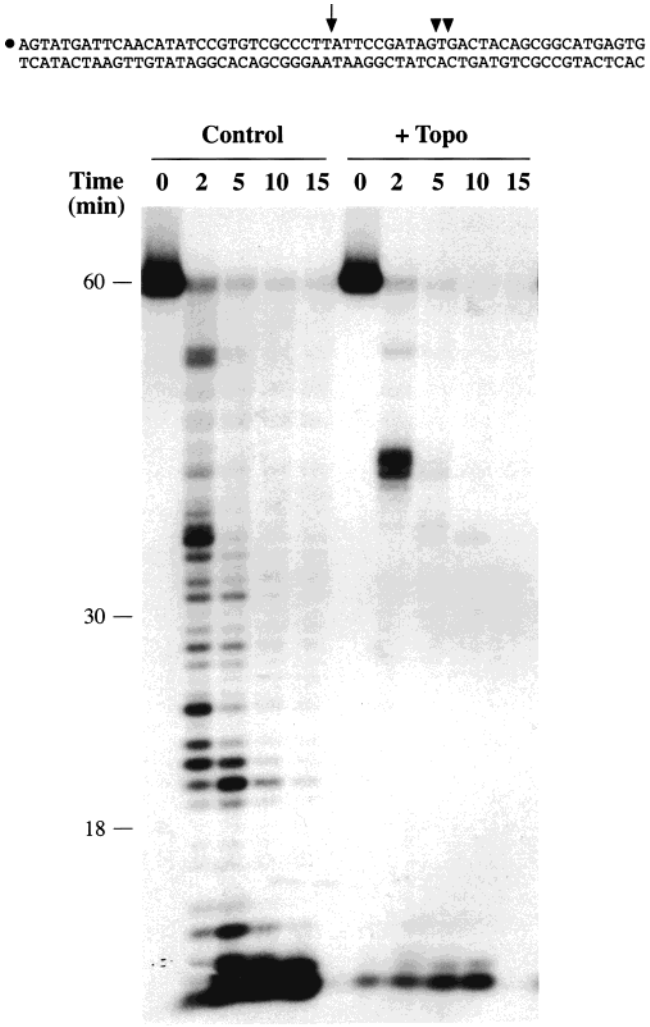

FIGURE 2: Exonuclease III footprint of vaccinia topoisomerase on the cleaved strand of CCCTT-containing duplex DNA. The structure of the 60-bp CCCTT-containing substrate is shown. The site of covalent adduct formation is indicated by a vertical arrow. The 5′ ^{32}P-label on the scissile strand is denoted by a dot. The margins of the exonuclease III footprint on the scissile strand are marked by arrowheads. Reaction mixtures (60 μL) containing 50 mM Tris HCl (pH 7.5), 1 mM $MgCl_2$, 3 pmol of DNA substrate, and 15 pmol of topoisomerase were incubated for 15 min at 22 °C. Control reaction mixtures lacking topoisomerase were incubated in parallel. Footprinting reactions and product analysis were performed as described in Figure 1. An autoradiograph of the polyacrylamide gel is shown. The positions and sizes of 5′-labeled DNA markers are indicated.

that exonuclease III digestion converts the equilibrium substrate to a suicide substrate as the segment of the scissile strand 3′ of the +1T is shortened to 11 nucleotides or less. It is well established that the cleavage reaction favors covalent adduct formation when the length of the duplex 3′ of the +1T is short enough to permit spontaneous dissociation of the leaving strand (*4*). Thus, the results in Figure 2 engender a clear conclusion that there is a footprint margin located 10−11 nucleotides downstream of the scissile phosphate. We would not be able to detect (and thus cannot exclude) the existence of an additional footprint margin closer to the +1T.

Kinetic Analysis of Single Turnover Cleavage Reveals the Catalytic Contribution of Phosphates and Bases Immediately 3′ of the CCCTT Target Site. Previous experiments indicated that as few as 6 bp upstream and 2 bp downstream of the scissile phosphate are sufficient to support covalent adduct formation between topoisomerase and CCCTT-containing duplex DNA (*3*). To determine quantitatively the contribution of specific DNA functional groups to the transesterification reaction (in particular the functional groups 3′ of the CCCTT sequence), we designed an array of nicked and gapped substrates shown in Figure 3. One subset of ligands (substrates A, B, and C) was composed of two 18-mer oligonucleotides annealed to a 60-mer complementary strand. A second subset (substrates D and E) was composed of one 18-mer CCCTT-containing strand annealed to the complementary 60-mer to yield a duplex with only one or two base pairs downstream of the scissile phosphate. Each substrate was 5′ radiolabeled on the strand containing the scissile phosphate. All other strands contained 5′ OH termini. Transesterification by topoisomerase on substrates A−E is expected to be a single-turnover reaction, i.e., covalent adduct formation results in dissociation of the leaving groups 5′-AT or 5′-A so that the enzyme becomes covalently trapped on the radiolabeled CCCTT-containing DNA strand. Covalent complex formation was revealed by transfer of the 5′ radiolabeled DNA to the topoisomerase polypeptide to form a protein−DNA adduct that was detectable by SDS−PAGE (*3*). The extent of strand cleavage was quantitated (as the percent of input labeled DNA transferred to protein at the reaction endpoint), and the apparent cleavage rate constant (k_{obs}) for each substrate was determined from a semilog plot of the approach to the endpoint. The results are summarized in Figure 3.

Substrate A can be viewed as a 36-bp duplex that lacks a single phosphate moiety at position −2. (The scissile phosphate Tp↓A is defined as the +1 phosphate.) Covalent adduct formation on substrate A proceeded to an extent of 93% of the input DNA. The amount of covalent adduct formed at 5 s was ~88% of the end-point value. We used this datum to estimate a rate constant of 0.4 s^{-1}. Substrate D contains only 2 bp of duplex DNA 3′ of the scissile phosphate, yet the extent of covalent adduct formation (86%) and the apparent cleavage rate constant (0.3 s^{-1}) were essentially the same as for substrate A. We conclude that moieties on the scissile strand 3′ of the −2T nucleoside make no significant contribution to the transesterification reaction on the 5′-tailed CCCTTAT-containing duplex.

Substrate B lacks a single phosphate at the −1 position. The effect of removing this phosphate is to reduce the apparent cleavage rate constant to 8.7×10^{-3} s^{-1}. The observed rate constant for substrate B did not increase when the concentration of topoisomerase in the reaction mixture was increased 2-fold (not shown). This suggests that a defect in initial binding of enzyme to ligand is not the cause of the slowed cleavage rate. Comparison of substrate B to substrate A engenders the conclusion that the −1 phosphate enhances the rate of transesterification by about a factor of 40.

Substrate C, which contains a 1-nucleotide gap, is missing the −1 phosphate *and* the −2T nucleoside. The cleavage rate constant for substrate C (3.5×10^{-4} s^{-1}) is about 1100-fold less than that of substrate A and about 25-fold less than that of substrate B. The rate of cleavage of substrate C did not increase when the concentration of topoisomerase in the reaction mixture was increased 2-fold (not shown), suggesting that a binding defect is not the cause of the slowed cleavage rate. The comparison between substrates C and B

Substrate		Cleavage	k obs (s^{-1})
A	TATCCGTGTCGCCCTTAT *tccgatagtgactacagc* TCATACTAAGTTGTATAGGCACAGCGGGAATA-AGGCTATCACTGATGTCGCCGTACTCAC	93%	0.4
B	ATATCCGTGTCGCCCTTA *ttccgatagtgactacag* TCATACTAAGTTGTATAGGCACAGCGGGAAT-AAGGCTATCACTGATGTCGCCGTACTCAC	72%	8.7×10^{-3}
C	ATATCCGTGTCGCCCTTA *tccgatagtgactacagc* TCATACTAAGTTGTATAGGCACAGCGGGAATAAGGCTATCACTGATGTCGCCGTACTCAC	72%	3.5×10^{-4}
D	TATCCGTGTCGCCCTTAT TCATACTAAGTTGTATAGGCACAGCGGGAATAAGGCTATCACTGATGTCGCCGTACTCAC	86%	0.3
E	ATATCCGTGTCGCCCTTA TCATACTAAGTTGTATAGGCACAGCGGGAATAAGGCTATCACTGATGTCGCCGTACTCAC	68%	5.9×10^{-5}

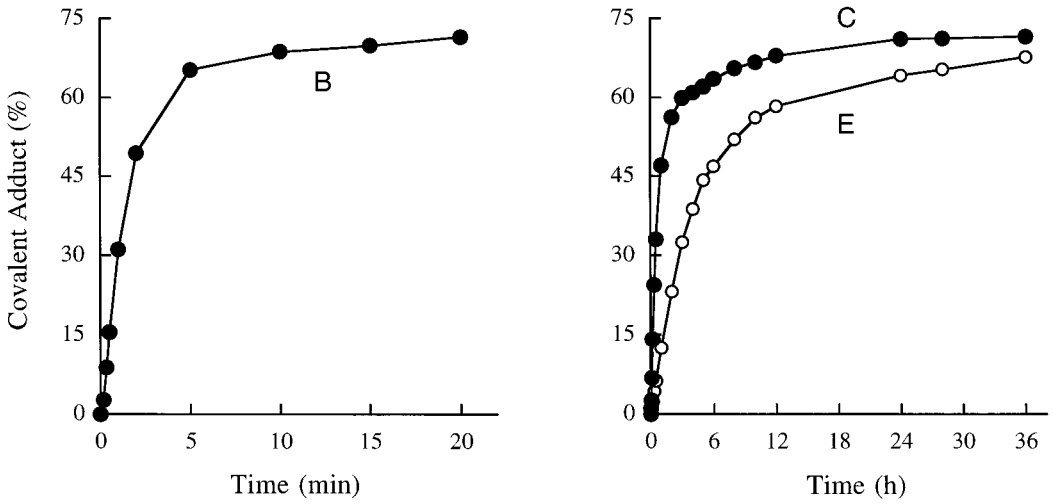

FIGURE 3: Kinetic analysis of the cleavage of substrates nicked and gapped downstream of the scissile phosphate. The structures of substrates A−E are shown with the site of covalent adduct formation indicated by an arrow. The 5′ ^{32}P-labeled 18-mer oligonucleotide containing the scissile phosphate (depicted in capital letters) was annealed to the 60-mer template strand and the downstream 18-mer component of the scissile strand (depicted in lower case letters) at a molar ratio of 1:4:4. Topoisomerase cleavage reaction mixtures containing (per 20 μL) 50 mM Tris HCl (pH 7.5), 0.5 pmol of 5′-labeled substrate DNA, and 2.5 pmol of topoisomerase were incubated at 37 °C. The reactions were initiated by the addition of enzyme. Aliquots (20 μL) were withdrawn at various times and quenched immediately by adding SDS to 1% final concentration. The samples were electrophoresed through a 10% polyacrylamide gel containing 0.1% SDS. DNA label-transfer to the topoisomerase was quantitated by scanning the dried gels with a FUJIX BAS2000 Phosphorimager. The accumulation of covalent adduct as a function of time is plotted for substrate B in the *left* panel and for substrates C and E in the *right* panel. The extents of covalent adduct formation at the reaction endpoints are shown next to each substrate. To determine the cleavage rate constants (k), the actual cleavage values at each time point were normalized to the endpoint value (redefined as 100) and the data were fit to the equation $100 - \%\text{cleavage}_{(\text{norm})} = 100\ e^{-kt}$. The observed rate constants are listed next to the substrates.

indicates that the −2T nucleoside contributes a 25-fold cleavage rate enhancement.

Substrate E lacks the −2 pT nucleotide present in substrate D. Removal of this nucleotide (consisting of the −1 phosphate plus the −2 nucleoside) reduces the cleavage rate constant to 5.9×10^{-5} s^{-1}. The observed rate constant for substrate E did not increase when the concentration of topoisomerase in the reaction mixture was increased 2- or 4-fold (not shown). The 5000-fold rate decrement on substrate E compared to substrate D is slightly greater than the 1100-fold rate disparity elicited by deleting the pT nucleotide in the three-stranded substrates (A versus C). The 6-fold rate difference between substrates C and E suggests that the segment of the scissile strand including and distal to the −3 nucleoside (this segment being present in C, but missing in E) *may* contribute to enhancement of the cleavage reaction when other key moieties are missing (in this case, the pT nucleotide at position −2).

Effects of Nicks within the CCCTT Motif. To explore the effects of strand discontinuity within the CCCTT target site, we introduced single nicks (composed of 3′ OH and 5′ PO_4 termini) at and immediately 5′ of the scissile phosphate. The position of the nick was sequentially phased in substrates F−K (Figure 4). Reaction of topoisomerase with substrates G−K resulted in label transfer from the 5′ end-labeled DNA strand containing the scissile TpA phosphodiester to the topoisomerase polypeptide to form a discrete covalent protein−oligonucleotide adduct that was resolved by SDS−PAGE (Figure 4, left panel). Note that the apparent size of the topoisomerase−DNA adduct increased in stepwise fashion as the length of the scissile strand 5′ of the TpA phosphodiester was increased from one to five nucleotides (Figure 4, left panel, lanes G−K). The covalent adduct formed with substrate K (predicted to contain a 5′-labeled pentanucleotide) migrated more rapidly than the adduct formed with a suicide substrate containing 12 nucleotides

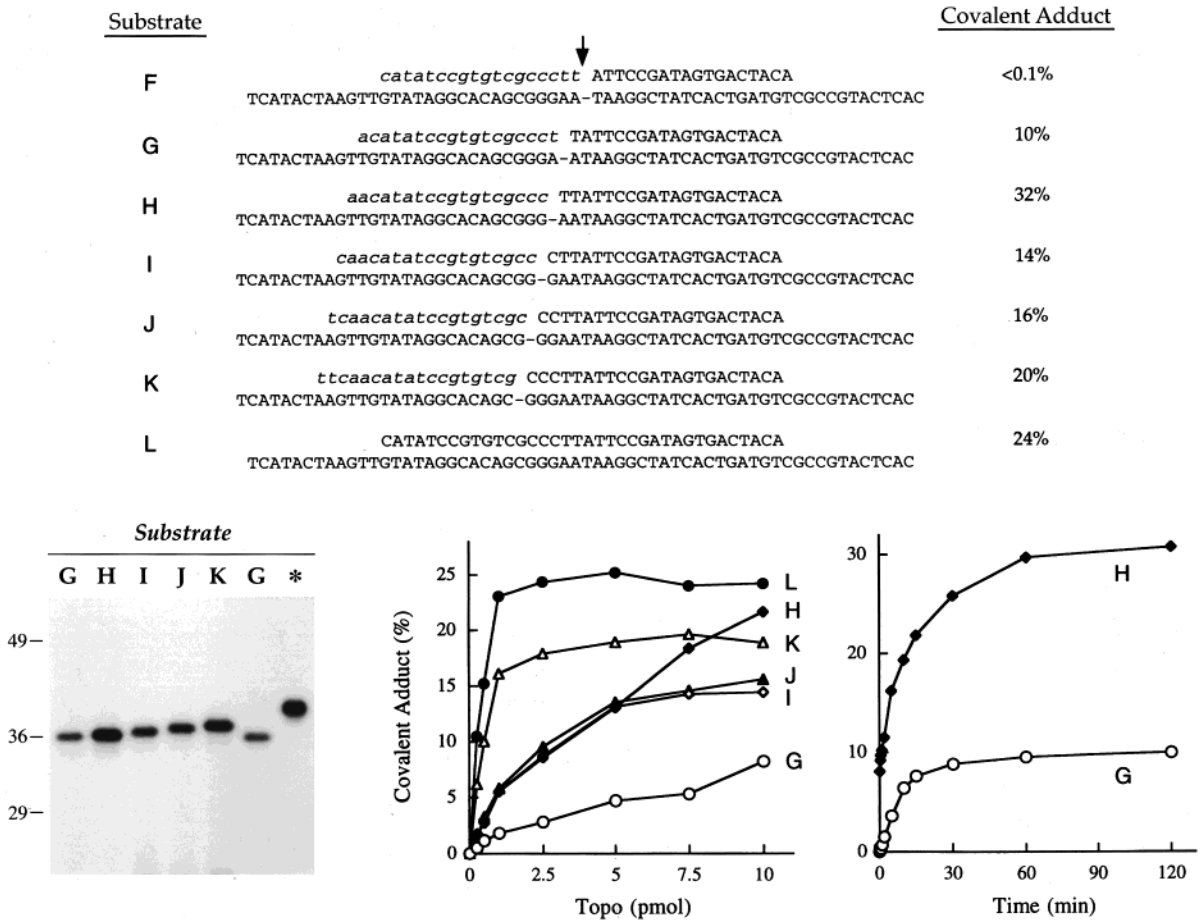

FIGURE 4: Cleavage of substrates containing nicks within CCCTT. The structures of substrates F−L are shown with the site of covalent adduct formation indicated by an arrow. The 5′ ^{32}P-labeled oligonucleotide containing the scissile phosphate (depicted in capital letters) was annealed to the 60-mer template strand and the upstream 18-mer component of the scissile strand (depicted in lower case letters) at a molar ratio of 1:4:4. (Left panel) Reaction mixtures (20 μL) containing 50 mM Tris HCl (pH 7.5), 0.5 pmol of radiolabeled substrate DNA as specified, and either 5 pmol of topoisomerase (substrates I, J, and K) or 10 pmol of topoisomerase (for substrates G and H) were incubated at 37 °C for either 15 min (I, J, K) or 2 h (G, H). The reaction mixture in the lane marked with an asterisk (*) contained 0.5 pmol of an 18-mer/30-mer suicide substrate containing the 5′-labeled scissile strand pCGTGTCGCCCTTATTCCC. The reactions were quenched with SDS and the products were analyzed by SDS−PAGE. An autoradiogram of the gel shown. The positions and sizes (in kilodaltons) of coelectrophoresed prestained marker proteins are indicated on the left. (Middle panel) Reaction mixtures containing 0.5 pmol of radiolabeled substrate DNA as indicated and topoisomerase as specified were incubated at 37 °C for 15 min. The reaction products were analyzed by SDS−PAGE. The dependence of covalent adduct formation on input enzyme is plotted for each substrate as indicated. (Right panel) Reaction mixtures containing (per 20 μL) 0.5 pmol of radiolabeled substrates G or H and 10 pmol of topoisomerase were incubated at 37 °C. Aliquots (20 μL) were withdrawn at the times indicated and quenched immediately with SDS. Covalent adduct formation is plotted as a function of reaction time. The yields of covalent adduct at the apparent kinetic endpoints under conditions of saturating input enzyme are annotated to the right of each substrate.

5′ of the scissile phosphate (Figure 4, left panel, lane *). We conclude that the substrates containing a nick within the CCCTT target site were cleaved by vaccinia topoisomerase at the same site to which transesterification occurs on a continuous scissile strand. On the other hand, we detected no label transfer to topoisomerase when the enzyme was reacted with substrate F at 5-fold enzyme excess over DNA for reaction times up to 29 h (not shown). We conclude that vaccinia topoisomerase is not capable of catalyzing transesterification to a 5′ monophosphate end, i.e., the enzyme is an obligate nucleic acid-transferase or nucleotidyl-transferase and not a phosphotransferase.

The reactivity of topoisomerase with the nicked substrates G−K was assessed in a more quantitative fashion and compared to the reactivity of the enzyme with an equilibrium substrate (L) composed of a 36-mer scissile strand with a centrally placed cleavage site. Note that the substrates are configured such that the 5′ OH leaving strand is 18 nucleotides in every case; thus, the extent of base pairing 3′ of the scissile phosphate is invariant and should not affect the reaction endpoints. The dependence of covalent adduct formation on input topoisomerase during a 15 min reaction is plotted for each substrate in Figure 4 (middle panel). Covalent adduct formation on the equilibrium substrate L (0.5 pmol/reaction) was enzyme dependent at substoichiometric levels of protein and plateaued between 1 and 10 pmol of topoisomerase with 24% of the DNA bound covalently ($K_{cl} \approx 0.3$). Substrate K, containing a nick between +6G and +5C, displayed similar enzyme dependence of covalent adduct formation (indicating that the strand interruption did not affect DNA site affinity), but attained a slightly lower extent of cleavage at saturation (20% covalent complex; $K_{cl} \approx 0.25$). Substrates J and I, with nicks at +5C/+4C and +4C/+3C, respectively, displayed a clear shift to the right in their titration curves, attaining saturation at 5−10 pmol of input topoisomerase, with 14−16% covalent adduct

formation (Figure 4). Thus, these strand discontinuities elicit an approximately 5-fold reduction in DNA-binding affinity. Substrates H and G, with nicks at +3C/+2T and +2T/+1T, respectively, displayed an even greater shift to the right of their enzyme dependence of covalent adduct formation, attaining saturation at 10−15 pmol of topoisomerase (Figure 4 and data not shown). We infer about a 10-fold affinity decrement for these strand breaks within the CCCTT target site.

Kinetic analysis of the cleavage of equilibrium substrate L and nicked substrates K, J, and I by saturating amounts of topoisomerase showed that in each case the reaction endpoint was attained in 10 s (the earliest time point tested; data not shown). The endpoint values in the kinetic experiments using these substrates agreed with the results of the protein titration experiments (not shown). However, the kinetics of covalent adduct formation on substrate H were dramatically different. Substrate H, with a +3C/+2T nick, displayed biphasic kinetics. The reaction entailed a rapid burst of cleavage at 10−60 s to a level of 8−10% covalent adduct formation, followed by a slow phase from 1 to 60 min, during which the level of covalent complex increased steadily from 10 to 30%. An apparent end point of 31% cleavage was attained at 120 min (Figure 4). The kinetic data are consistent with the rapid establishment of a cleavage-religation equilibrium (the burst phase), followed by slow dissociation of the topoisomerase-dinucleotide adduct, pTpTp-(Topo), from the DNA to establish a new equilibrium involving the binding and dissociation of pTpTp-(Topo). The results with substrate H suggest that either base-pairing interactions of the scissile and nonscissile strands within the CCCTT target site or specific contacts of topoisomerase with the (+3C)p-(+2T) phosphodiester are important in stabilizing the topoisomerase−DNA interaction even *after* the covalent adduct is formed.

Substrate G, with a nick at +2T/+1T, displayed an apparent first-order approach to equilibrium over 15 min, attaining an endpoint of 10% covalent complex. The apparent rate constant for approach to equilibrium was 0.0014 s^{-1}, which is slower by a factor of at least 500 than the rate constant for covalent adduct formation on a standard equilibrium substrate. A simple interpretation of the slow rate on substrate G would be that the nick at +2T/+1T directly impedes transesterification chemistry (even though the nick itself is not chemically reactive during attack on the neighboring scissile phosphate), but ultimately permits establishment of a cleavage religation equilibrium with $K_{cl} \approx 0.1$. We do not exclude an alternative model in which an initial rapid equilibrium of substrate G (with a much lower K_{cl} caused by a drastic reduction in the rate of strand cleavage relative to religation) is followed by a second phase of slow dissociation of the topoisomerase-mononucleotide complex.

Effects of Missing-Phosphate Nicks within 3′-GGGAA of the Nonscissile Strand. A series of substrates missing single phosphates in the nonscissile strand is shown in Figure 5 (substrates M−R). These DNAs were prepared by annealing a 5′-radiolabeled 60-mer scissile strand containing a centrally placed CCCTT cleavage site to two complementary 18-mer oligonucleotides to create a 36-bp duplex segment with a 3′-OH/5′-OH strand discontinuity. Cleavage reactions were performed by incubating the substrates with a 5-fold molar excess of topoisomerase. The reactions were quenched with SDS. After proteinase K digestion to remove covalently linked topoisomerase, the radiolabeled DNA reaction products were analyzed by denaturing polyacrylamide gel electrophoresis (Figure 5).

Reaction of topoisomerase with substrate M, which lacked the phosphate opposite the scissile phosphate (we will refer to this as the +1 phosphate of the nonscissile strand), resulted in the appearance of radiolabeled species, migrating at ∼32−34 nucleotides, that correspond to the expected 30-mer cleavage product linked to one or more amino acids of the topoisomerase (Figure 5, lane M+). An additional discrete labeled species was observed with an apparent mobility of 48 nucleotides. Detection of the covalent oligonucleotide−peptide complex was completely dependent on prior digestion of the sample with proteinase K (Figure 5, compare lanes M+ and M−). This is because the labeled DNA does not migrate into the polyacrylamide gel when it is bound covalently to the topoisomerase polypeptide. In contrast, the 48-mer product was present in equal abundance with or without proteinase K treatment (Figure 5). This indicated that the 48-mer corresponds to a novel DNA ligation product that is not covalently bound to the topoisomerase. Quantitation of the product distribution after a 30 min reaction showed that 75% of the input 60-mer scissile strand was converted to covalent adduct, while 6% was converted to the recombinant species. Thus, a total of 81% of the substrate had undergone transesterification. The extent of transesterification on substrate M is higher than that on an equilibrium substrate because (i) CCCTT strand scission results in a blunt-end double-strand break and (ii) the downstream cleavage product is not tightly held by the enzyme in the absence of tethering to a continuous complementary strand. Kinetic analysis of the reaction with substrate M showed that 65% of the scissile strand became covalently linked to topoisomerase in 5 s, at which time the recombinant species comprised only 1% of the labeled DNA (Figure 6). An apparent rate constant for covalent adduct formation of 0.39 s^{-1} was calculated from this datum. This value was quite close to the observed rate constant for cleavage of a suicide substrate. We infer that the transesterification reaction of vaccinia topoisomerase on duplex substrate M is not adversely affected by the lack of a phosphate opposite the scissile phosphate.

Reaction of topoisomerase for 30 min with substrate N, which is missing the +2 nonscissile strand phosphate, resulted in conversion of 46% of the input labeled strand to a covalent protein−DNA adduct and 20% to a 48-mer recombinant species (Figure 5, lane N). The recombinant 48-mer was evident whether or not the products were treated with proteinase K, whereas the oligonucleotide−peptide adduct was seen only when the products were treated with proteinase K (Figure 5, compare lane N+ and N−). The kinetics of the reaction are shown in Figure 6. Covalent adduct formation was virtually complete in 10 s (the earliest time point tested) and plateaued at 20−60 s with 60% of the input 60-mer covalently bound to topoisomerase. (This adduct is predicted to contain a single T overhang if the 3′ cleavage product is released from the topoisomerase−DNA complex.) Thus, removal of the +2 phosphate on the complementary strand has no apparent effect on transesterification rate. The recombinant species comprised 4% of the labeled DNA at 10−30 s and then increased steadily to 20%

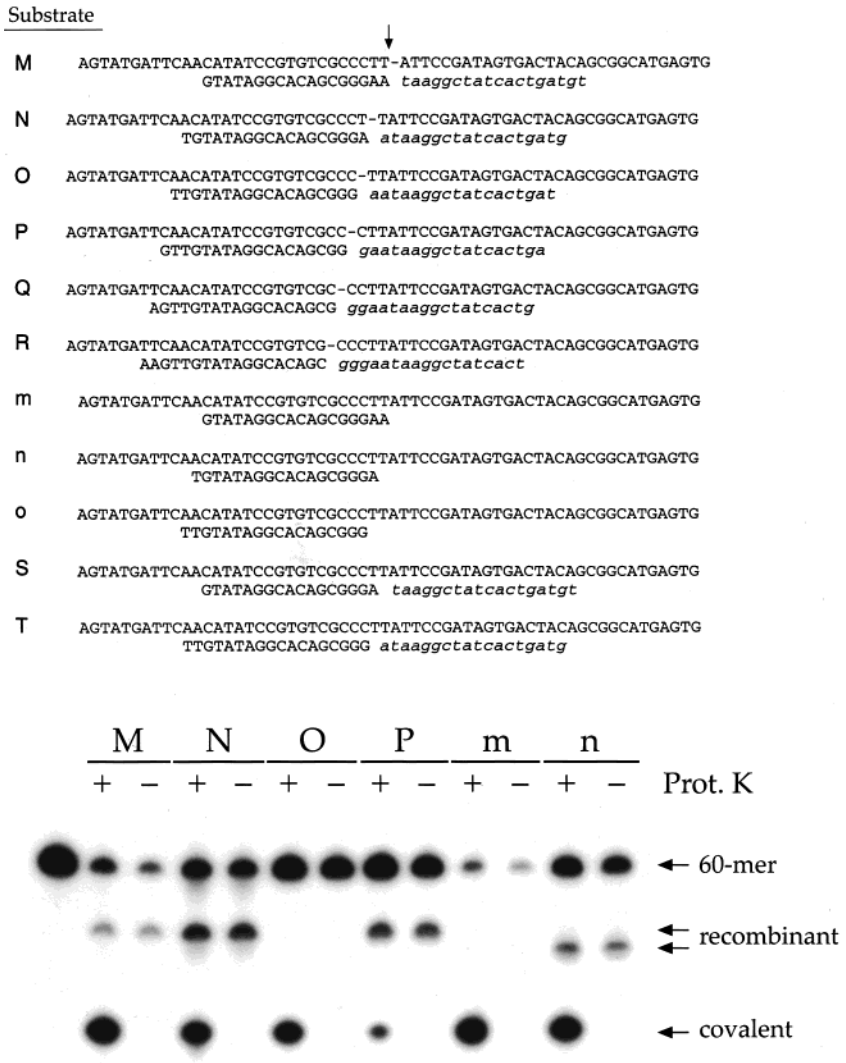

FIGURE 5: Cleavage of substrates containing nicks and gaps in the nonscissile strand. Substrates M−T were formed by annealing the 5′ ^{32}P-labeled 60-mer scissile strand to two complementary 18-mer oligonucleotides at a molar ratio of 60-mer/18-mer/18-mer of 1:4:4. Substrates m−o were formed by annealing the labeled 60-mer to one complementary 18-mer strand at a molar ratio of 1:4. The structures of the substrates are shown. The two 18-mer oligonucleotides that comprise the bottom strand are depicted in different type face for the sake of clarity. Reaction mixtures containing (per 20 μL) 50 mM Tris HCl (pH 7.5), 0.5 pmol of labeled DNA substrate, and 2.5 pmol of topoisomerase were incubated for 30 min at 37 °C. Duplicate aliquots (20 μL) were withdrawn and quenched with SDS. One sample was digested with 10 μg of proteinase K for 60 min at 37 °C (lanes +) while the other sample from each pair was not subjected to proteolysis (lanes −). The DNA was recovered by ethanol precipitation. The pellets were resuspended in formamide and the samples were analyzed by electrophoresis through a 11% polyacrylamide gel containing 7 M urea in TBE. An autoradiogram of the gel is shown. The positions of the input ^{32}P-labeled 60-mer CCCTT-containing strand (60-mer), the covalent 30-mer/peptide adduct (covalent), and the DNA strand transfer products (recombinant) are indicated by arrows on the right.

during the period from 60 s to 30 min, concomitant with a gradual decline in the level of the covalent adduct. The biphasic kinetic data indicate that the recombinant species is derived from the covalent topoisomerase−DNA complex via a slow phase of religation to a 5′ OH strand other than the 30-mer leaving strand generated during the initial cleavage reaction. Further characterization of the recombinant species showed that the 5′-OH terminus of the distal 18-mer oligonucleotide of the nonscissile strand acts as the nucleophile in the strand transfer reaction (see below).

Reaction of topoisomerase with substrate O, which is missing the +3 phosphate on the nonscissile strand, yielded 35% covalent adduct, but resulted in only trace levels of strand transfer to generate a recombinant species (Figure 5). The covalent adduct on substrate O is predicted to contain a TT dinucleotide overhang if the noncovalently held cleavage product is released from the topoisomerase−DNA complex. The finding that the extents of transesterification are progressively lower on substrates M, N, and O, which correlates with the transition from a blunt-end cleavage product to a 1-nucleotide overhang to a 2-nucleotide overhang, suggests that base pairing might stabilize the noncovalently held DNA duplex on the topoisomerase−DNA complex after the scissile strand had been incised to generate a staggered double-strand break. In effect, the overhangs may confer some attributes of an equilibrium substrate. In the case of substrate O, the covalent adduct accumulated with apparent first-order kinetics and an apparent rate constant of 0.22 s^{-1} for approach to the end point (data not shown). There is some uncertainty whether this value represents an approach to equilibrium

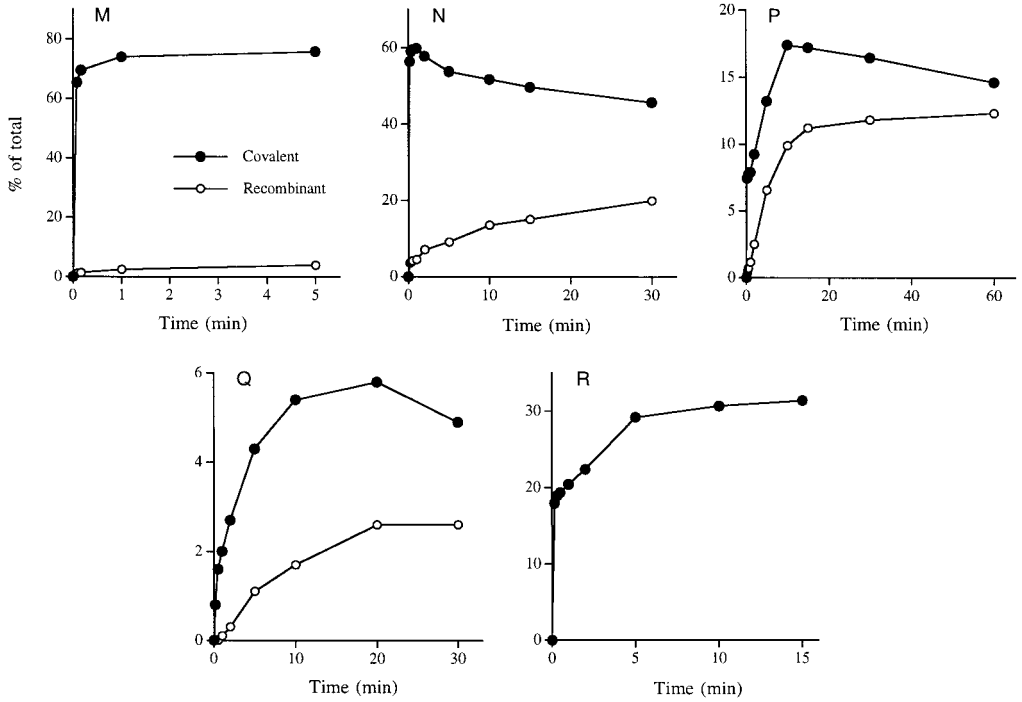

FIGURE 6: Kinetics of the reaction of topoisomerase with substrates containing missing-phosphate nicks in the nonscissile strand. Reaction mixtures containing (per 20 μL) 50 mM Tris HCl (pH 7.5), 0.5 pmol of substrates M, N, P, Q, or R, and 2.5 pmol of topoisomerase were incubated at 37 °C. The reactions were initiated by the addition of topoisomerase to prewarmed mixtures containing DNA. Aliquots were withdrawn at the times specified and the reaction was quenched immediately by adding SDS to 0.5%. The samples were processed and analyzed as described in Figure 5. The levels of the covalent 30-mer/peptide adduct (covalent), and the DNA strand transfer product (recombinant) were expressed as percent of total labeled DNA and plotted as a function of reaction time.

(equivalent to the sum of the cleavage and religation rates) or a single-turnover cleavage rate. In either event, we surmise that elimination of the +3 phosphate of the nonscissile strand has a modest effect on the rate of transesterification (an estimated 2-fold decrement if single-turnover and a 5-fold decrement if the rate is an approach-to-equilibrium).

Kinetic analysis of the reaction of topoisomerase with substrate P, which is missing the +4 phosphate on the nonscissile strand, revealed three distinct phases. Topoisomerase converted 7% of the input 60-mer to the covalent adduct in 10 s. The covalent complex persisted at this level for 60 s, then increased to 17% over 1−10 min, before decaying slowly from 10 to 60 min (Figure 6). The recombinant species increased from 10 s to 10 min (following the initial burst of covalent adduct formation and roughly paralleling the second slow phase of covalent adduct formation) to a level of 10% of the labeled DNA and then accumulated more slowly from 15 to 60 min, concomitant with the decline in covalent adduct (Figure 6). A plausible scenario for the triphasic pattern entails (i) rapid establishment of an equilibrium cleavage complex stabilized by the trinucleotide overhang of the staggered double-strand break; (ii) slow dissociation of the noncovalently held cleavage product to yield covalent adduct with a trinucleotide overhang; (iii) strand transfer by the covalent adduct containing the trinucleotide overhang to the 18-mer component of the nonscissile strand to form the 48-mer recombinant.

Topoisomerase was very poorly reactive with substrate Q, which is missing the +5 phosphate on the nonscissile strand. The covalent adduct accumulated slowly over 10 min to ~5% of the total DNA (Figure 6). The formation of the recombinant species lagged behind that of the covalent intermediate, as expected, and the recombinant was <3% of total labeled DNA after 30 min. The kinetic profile, plus the fact that the extent of reaction with substrate Q was significantly lower than the endpoint on a fully duplex equilibrium substrate, suggested that elimination of the +5 phosphate impaired cleavage chemistry.

Transesterification activity was substantially restored on substrate R, in which the missing phosphate was phased to position +6 on the nonscissile strand. The reaction entailed a burst of 18% covalent adduct formation in 10 s, followed by a slow increase in covalent adduct over 5 min (Figure 6). The reaction plateaued with 31% covalent adduct at 15 min, with no detectable formation of a recombinant species. These findings were consistent with the rapid establishment of a cleavage-religation equilibrium on substrate R, followed by slow dissociation of the noncovalently held cleavage product.

In summary, the effects of introducing missing phosphate nicks on the nonscissile strand suggest that (i) base-pairing interactions on the 3′-GGGAA side of the scissile phosphate contribute to the stability of the cleaved complex; (ii) topoisomerase bound covalently to a 3′ overhang is recombinogenic; and (iii) the +5 phosphate (3′-G**p**GGAA) of the nonscissile strand is specifically important for transesterification.

Characterization of the Strand-Transfer Product. The ~48-nucleotide 5′-labeled recombinant strand generated by topoisomerase in its reaction with substrate N (Figure 5) was purified by preparative gel electrophoresis and then subjected to Maxam−Gilbert chemical sequencing. The sequence of this molecule across the strand-transfer junction was 5′-GCCCTTGTAGTCACTAT. Thus, the 48-mer arose via

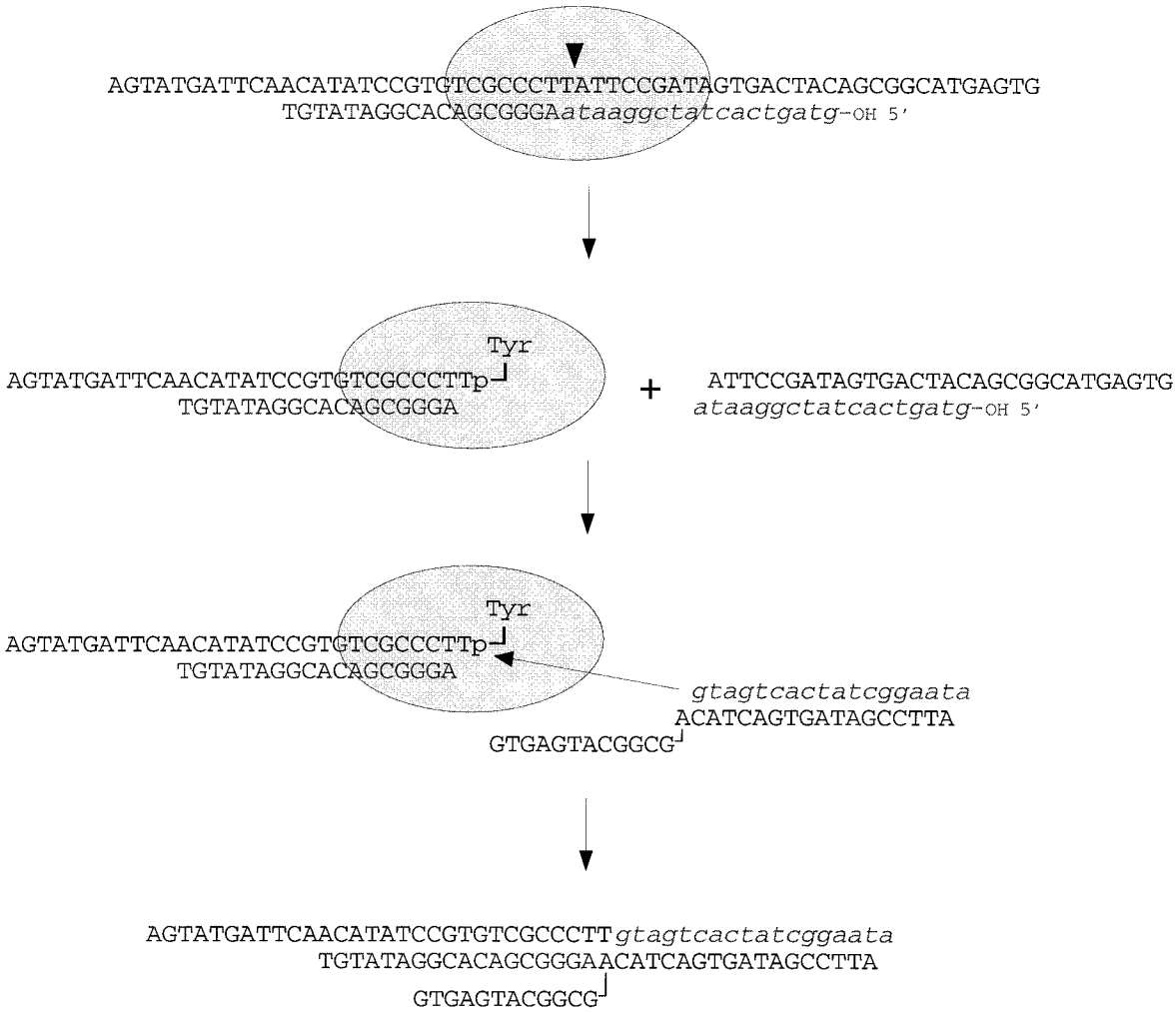

FIGURE 7: Strand transfer by topoisomerase at a 3′ overhang. The pathway of strand transfer on substrate N is illustrated as a series of component steps: (1) transesterification of Tyr-274 to the CCCTT↓A site resulting in dissociation of the distal duplex and covalent attachment of topoisomerase at a 3′ T overhang; (2) rebinding of the released cleavage product in the inverted orientation such that the 5′-OH of the terminal guanosine of the 18-mer strand is poised for nucleophilic attack on the CCCTTp-Tyrosine phosphodiester; (3) religation to form a novel molecule containing a "recombinant" 48-mer CCCTT top strand and 3′ single strand "flap" on the bottom strand. Note that the 48-mer can also be formed by attack of the 18-mer strand of intact substrate N on the covalent adduct containing a 3′ overhang.

transfer of the covalently held 5′ 30-nucleotide segment of the input scissile strand to the 5′-OH terminus of the 18-mer component of the noncovalently held cleavage product. A likely strand transfer reaction scheme is illustrated in Figure 7. The key element is that the 3′ cleavage product can religate either to the CCCTT strand in the original orientation, in which case the original labeled 60-mer would be reconstituted, or in an inverted orientation, resulting in the appearance of a novel recombinant. Note that we cannot determine from the product analysis whether the level of intact 60-mer strand present at the reaction endpoint represents unreacted substrate or a population of molecules that have undergone cleavage and religation. Religation by the covalent CCCTT-Topo intermediate formed on substrate N, which contains a single unpaired 3′ T overhang at the +1 position (Figure 7), might be biased in favor of an "acceptor" DNA molecule that has the capacity to form a base pair with the T overhang. Indeed, this scenario may account for the high level of recombinant accumulation on substrate N, because the 3′ single-strand tail of the inverted downstream cleavage product of substrate N has an unpaired A immediately flanking the 5′-OH guanosine of the attacking strand (Figure 7). Similarly, substrate P, which is also recombinogenic, contains an unpaired A flanking the 5′-OH of the 18-mer component of the duplex leaving group.

Effects of Incremental 5′-Deletions into the 3′-GGGAA Element of the Nonscissile Strand. To gauge the contribution of the nucleotides within the 3′-GGGAA element to the topoisomerase transesterification reaction, we constructed substrates m, n, and o (Figure 5). These molecules were formed by annealing the 5′-labeled 60-mer scissile strand to a single complementary 18-mer such that the 5′ margin of the duplex segment either extended to position +1 (in substrate m) or was phased leftward to positions +2 (substrate n) or +3 (substrate o). Substrates m, n, and o are related to M, N, and O in that the lower case substrates lack the rightward (italicized) 18-mer components of the complementary strands used to form the upper case substrates (Figure 5). Reaction of topoisomerase with substrate m resulted in the conversion of 87% of the input labeled DNA to covalent adduct in 5 min (Figure 8). Detection of the 30-mer/peptide adduct again depended on digestion of the reaction products with proteinase K (Figure 5; lanes m+ and m−). The apparent cleavage rate constant for substrate m

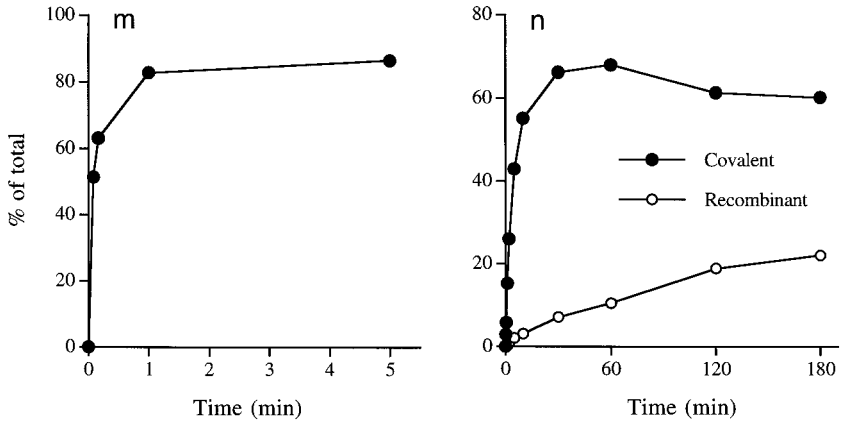

FIGURE 8: Kinetics of the reaction of topoisomerase with substrates containing deletions in the 3′-GGGAA element of the nonscissile strand. Reaction mixtures containing (per 20 μL) 0.5 pmol of substrates m or n and 2.5 pmol of topoisomerase were incubated at 37 °C. The levels of the covalent 30-mer/peptide adduct (covalent), and the DNA strand transfer product (recombinant) were expressed as percent of total labeled DNA and plotted as a function of reaction time.

was 0.18 s^{-1}. A comparison to the rate constants for substrates m and M engenders the conclusion that the complementary strand to the right of the cleavage site makes only a modest (2-fold) contribution to the rate of transesterification to a 60-mer scissile strand that is otherwise fully base paired within the CCCTT sequence.

Phasing the 18-mer duplex segment one position to the left to leave an unpaired +1T in substrate n had a dramatic effect on the rate of transesterification. The reaction of topoisomerase with substrate n resulted in the conversion of 68% of the input 60-mer strand to the covalent adduct in 1 h followed by a slight decline to 60% after 3 h (Figure 8). A protein-free strand transfer product (Figure 5, lane n+ versus n−) also accumulated slowly over the 3 h reaction, at which point the recombinant species constituted 22% of the labeled material (Figure 8). A semilog plot of the accumulation of the covalent adduct from 10 s to 2 min (during which time the recombinant species did not contribute significantly to the overall extent of substrate decay) yielded an apparent rate constant of 0.0033 s^{-1}. A comparison to substrate m indicated that the elimination of the 3′-pA nucleotide opposite the +1T in the cleaved strand slowed the rate of transesterification by a factor of 50. The strand transfer product formed on substrate n migrated slightly faster during polyacrylamide gel electrophoresis than the recombinant molecule generated during the reaction of topoisomerase with substrate N (Figure 5). The only available DNA nucleophile for strand transfer after transesterification of the topoisomerase to substrate n is the 5′-OH 18-mer oligonucleotide comprising the complementary strand. Although we cannot discern from this experiment whether strand transfer occurs via an intramolecular or an intermolecular religation reaction, it is clear that the recombinant strand will form a hairpin structure once denatured. We reported previously that such hairpins migrate faster during polyacrylamide gel electrophoresis than expected from their chain length (*8*).

Phasing the 18-mer duplex segment one position farther to the left in substrate o, such that the +2T and +1T of the scissile strand are both unpaired, effectively abolished transesterification by topoisomerase, i.e., we detected no formation of covalent adduct during a 15 h reaction in topoisomerase excess (not shown). Did deletion of the +2T abolish transesterification per se or did it exacerbate the already deleterious effects of the +1A deletion on the topoisomerase reaction? To answer this question, we tested the effects of single nucleotide gaps at +1 and +2 in the nonscissile strand.

Effects of Single Missing Nucleotides within the 3′-GGGAA Element of the Nonscissile Strand. Substrate S consists of the scissile 60-mer annealed to two 18-mer strands to yield a gapped duplex molecule that is missing the +1A nucleoside and the flanking +1 and +2 phosphates on the nonscissile strand, but which is otherwise base paired over 18 nucleotide segments on either side of the gap (Figure 5). The reaction of topoisomerase with substrate S resulted in the conversion of 71% of the input 60-mer strand to the covalent adduct in 15 min (Figure 9). Two strand transfer products accumulated much more slowly, together comprising 6% of the labeled DNA after 15 min (Figure 9). The slower-migrating component of the doublet comigrated with the 48-mer recombinant strands formed in the reaction with substrates M and N, whereas the faster component in the doublet displayed the same electrophoretic mobility as the hairpin molecule formed with substrate n (not shown). Thus, the covalent intermediate formed on substrate S can religate to either of the 18-mer oligonucleotides that comprise the nonscissile strand. The apparent rate constant for covalent adduct formation on substrate S was 0.018 s^{-1}. This value is 5-fold greater than the rate observed for substrate n, which lacks the 18-bp duplex flanking the cleavage site. It appears that whereas the segment of the nonscissile strand to the right of the cleavage is not critical for transesterification when the CCCTT element is fully duplex (compare M versus m as discussed above), this segment can play a more substantial role when key moieties are lacking on the covalently held side of the target site (S versus n). A comparison of the rate constants for substrates M (0.39 s^{-1}) and S (0.018 s^{-1}), which differ only in the presence of absence of the 3′-pA nucleotide opposite the +1T on the scissile strand, indicates that this nucleotide enhances the reaction rate by a factor of 20. Given that the elimination of the nonscissile strand +2 phosphate alone had little effect on the rate of covalent adduct formation (substrate N), we surmise that loss of the +1T:A base pair is principally responsible for the rate decrement in substrate S.

Substrate T consists of the scissile 60-mer annealed to two 18-mer strands to yield a gapped duplex molecule that is

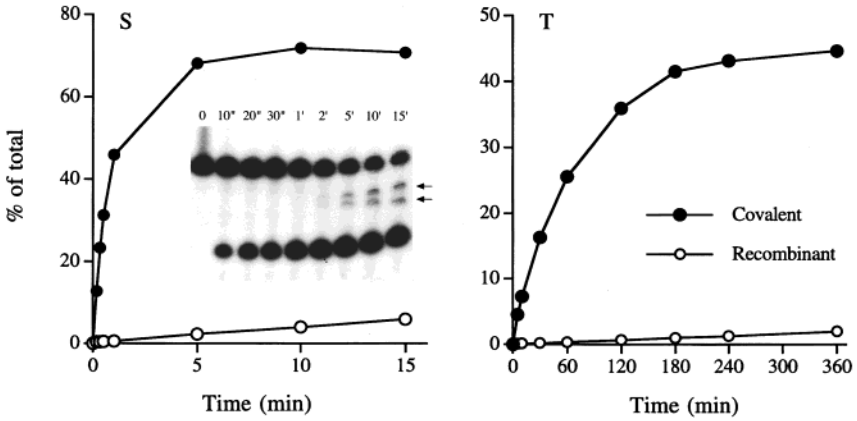

FIGURE 9: Kinetics of the reaction of topoisomerase with substrates containing 1-nucleotide gaps in the 3′-GGGAA element of the nonscissile strand. Reaction mixtures containing (per 20 μL) 0.5 pmol of substrates S or T and 2.5 pmol of topoisomerase were incubated at 37 °C. The levels of the covalent 30-mer/peptide adduct (covalent) and the DNA strand transfer product (recombinant) were expressed as percent of total labeled DNA and plotted as a function of reaction time. The insert in panel S is an autoradiogram showing an electrophoretic analysis of product formation on substrate S. The two recombinant species are indicated by arrows.

missing the +2A nucleoside and the flanking +2 and +3 phosphates on the nonscissile strand (Figure 5). The reaction of topoisomerase with substrate T resulted in the conversion of 45% of the input 60-mer strand to the covalent adduct in 6 h (Figure 9). A 48-nucleotide transfer product comprised 2% of the labeled DNA after 6 h. The apparent rate constant for covalent adduct formation on substrate T was 2.4×10^{-4} s^{-1}. Comparison to the rate constant for substrates O (0.22 s^{-1}), which differs from substrate T only in the presence or absence of the A nucleotide opposite the +2T on the scissile strand, indicates that this nucleotide enhances the reaction rate by 3 orders of magnitude. Again, given that removal of the nonscissile strand +2 phosphate alone has little effect on the rate of covalent adduct formation (substrate N), we surmise that loss of the +2T:A base pair is principally responsible for the large rate decrement in substrate T.

DISCUSSION

Topoisomerase-Binding Site on DNA. Exonuclease III footprinting experiments suggest a two-part interaction of topoisomerase with the DNA 5′ of the site of covalent adduct formation. A transient margin of protection from exonuclease III digestion, which extends to positions +13 to +14 on the scissile strand, gives way to a long-lived margin of protection at positions +7 to +9. The tightly protected segment includes the entire CCCTT↓ element that directs site-specific transesterification. Multiple points of contact within this segment have been inferred from modification protection, modification interference, and UV cross-linking approaches. We have shown that 6 bp of duplex DNA 5′ of the scissile phosphate are *sufficient* for transesterification by vaccinia topoisomerase on a suicide substrate (*3*). What then is the significance of the upstream footprint extending to +13/+14? Available data indicate that this segment contributes to the strength of noncovalent binding of topoisomerase to the CCCTT target site (*4*). There is also ample evidence that the affinity of the poxvirus topoisomerase for the pentapyrimidine motif and the extent of cleavage at equilibrium are affected by the DNA sequence context flanking the CCCTT element (*2*, *27*). The binding of topoisomerase to the CCCTT target site in the sequence context used in this and earlier studies results in strong protection of the +6G and +9G bases on the scissile strand from modification by dimethyl sulfate (*17*). Thus, the topoisomerase contacts the major groove at the border between the inner and outer footprints defined by exonuclease III. Changing the DNA sequence from +9 to +11 can negatively affect the cleavage-religation equilibrium (*27*). Thus, the contacts over the outer exonuclease III footprint, though not required for transesterification, can modulate the balance of cleavage and rejoining, presumably by influencing a proposed precleavage conformational step (*1*).

Scissile Strand. The kinetic contributions of the downstream portion of the scissile strand have been defined by studying the effects of nicks and gaps 3′ of the CCCTT sequence. We find that the −1 phosphate and −2 nucleoside enhance the rate of transesterification by factors of 40 and 25, respectively. The portion of the scissile strand downstream of the −2 nucleotide makes no significant contribution to the rate of cleavage, provided that there are two nucleotides present 3′ of the CCCTTp↓ site. We presume that the −1 phosphate and −2 nucleoside make contacts with amino acids on the enzyme; however, the sites of such contacts on the vaccinia topoisomerase cannot be surmised from the structure of the free catalytic domain (*20*). There are protein main-chain and side-chain contacts to the corresponding phosphate and nucleoside base downstream of the scissile phosphate in the DNA cocrystal structures of human topoisomerase I (*21*). However, the kinetic contributions of these DNA phosphate and nucleoside moieties to transesterification by human topoisomerase I have not been determined. Henningfeld and Hecht (*28*) noted that when mammalian topoisomerase I was reacted with a tailed substrate containing only 1 bp downstream of the intended scissile phosphate (analogous to substrate E in the present study), the enzyme failed to cleave at the expected site and instead cleaved at an alternative site 2 nucleotides upstream. Reaction with a substrate containing a nick at position −1 of the scissile strand (analogous to our substrate B) permitted some transesterification to the intended scissile phosphate, but most of the cleavage activity of the cellular enzyme was still diverted to the alternative site (*28*). Low yields of covalent adduct and the tendency of the cellular enzyme to switch sites when presented with modified DNA substrates make it difficult to perform and interpret kinetic experiments with

the cellular topoisomerase of the type conducted here with the stringently site-specific vaccinia virus enzyme.

Introduction of a 5′-phosphate/3′-OH nick in lieu of the scissile phosphodiester abolished transesterification by vaccinia topoisomerase, but did not affect the noncovalent binding of topoisomerase to the nicked DNA, as guaged by a native gel mobility-shift assay (J. Sekiguchi, unpublished results). This result indicates that vaccinia topoisomerase is an obligate polynucleotidyl-3′-phosphotransferase or nucleotidyl-3′-phosphotransferase. The enzyme apparently cannot transesterify to a 5′ phosphomonoester.

Placement of a 5′-phosphate/3′-OH nick at positions +2, +3, +4, and +5 within the CCCTT element resulted in a 5−10-fold reduction in the affinity of topoisomerase binding to DNA, as reflected in a shift in the enzyme dependence of covalent adduct formation. A nick at position +6 had no apparent effect on binding. The present results for single phosphate modifications agree with and extend our earlier studies showing that ethylation of phosphates +2, +3, and +4 on the scissile strand interfered with topoisomerase binding to DNA (*18*). Amino acid side chains within the crystal of vaccinia topoisomerase coordinate two sulfate ions in positions likely to be occupied by the +1 and +2 phosphates of the CCCTT strand (*20*). The sulfate corresponding to the +2 phosphate interacts with the guanidinium moiety of Arg-84, which has been shown through mutational analysis to be involved in the noncovalent binding of vaccinia topoisomerase to the DNA target site (*29*). The +2 phosphate in the human topoisomerase−DNA cocrystal interacts with the ϵ-amino group of Lys-443 (*21*). A structure-based alignment shows that Lys-443 in the human protein corresponds to Arg-84 in the vaccinia topoisomerase. Other potential interactions with the +3, +4, and +5 phosphates cannot be surmised from the structure of the free vaccinia enzyme. However, contacts between side-chain and main-chain groups of the human topoisomerase I and the +3, +4, and +5 scissile strand phosphates are evident in the DNA cocrystals of the human enzyme (*21*). The scissile strand +5 phosphate in the human topoisomerase−DNA complex interacts with the side-chain hydroxyl of Tyr-426 (*21*). The equivalent residue in the vaccinia topoisomerase structure (Tyr-70) interacts with the major groove of the CCCTT target site such that it can be cross-linked to the +4C base (*19*); in this position, Tyr-70 would also be in proximity to the +5 phosphate of the scissile strand. Changing Tyr-70 to alanine slows the cleavage rate constant by a factor of 3 and reduces the affinity of the topoisomerase for the DNA target site (*29*). The functional contributions of the +2, +3, +4, and +5 scissile strand phosphates to binding and catalysis, and the effects of mutations in amino acids that contact these moieties on binding and catalysis have not been reported for the human enzyme.

A nick at the +2 phosphate slowed the rate of transesterification by vaccinia topoisomerase some 500-fold (substrate G). This finding, together with earlier studies of the effects of position-specific base and sugar substitutions (*3*, *17*) and permanganate oxidation (*24*) on topoisomerase binding and transesterification, points to the +2 Tp nucleotide as being the most critical element of the CCCTT target site other than the scissile phosphate itself.

Nonscissile Strand. The segment 5′ of the 3′-GGGAA sequence contributes minimally to the rate of transesterification on the 60-mer CCCTT-containing strand provided that the substrate is otherwise fully base paired within the CCCTT sequence. By studying the effects of nicks within the 3′-GGGAA, we discerned an important role for the +5 phosphate in transesterification. This result is consistent with previous phosphate ethylation interference data that suggested a functional contact between vaccinia topoisomerase and the +5 phosphate of the nonscissile strand (*18*). Pourquier et al. (*30*) have analyzed the effects of missing-phosphate nicks in the nonscissile strand on DNA cleavage by human topoisomerase I. They found that a nick at position +5 in the nonscissile strand (numbered according to our nomenclature) suppressed transesterification, even in the presence of camptothecin, which would have trapped any covalent adduct that did form on the +5 nicked ligand (*30*). Thus, the poxvirus and human topoisomerases are both extremely sensitive to elimination of the +5 phosphate on the nonscissile strand. In the human topoisomerase−DNA cocrystal, there are four different points of contact between the protein and the +5 phosphate of the nonscissile strand involving two main-chain and two side-chain atoms (*21*). A test of the functional significance of the side-chain contacts to the +5 phosphate by mutagenesis of the human topoisomerase has not been reported.

Missing phosphate nicks at the +1, +2, +3, +4, and +6 positions of the nonscissile strand had no major effects on the kinetics of the initial burst of covalent adduct formation by vaccinia topoisomerase when assayed under conditions of enzyme excess. (These modifications did influence the amplitude of the burst, as noted in the Results.) Prior studies showed that ethylation of the nonscissile strand +3 and +4 phosphates interfered with vaccinia topoisomerase binding to DNA. It is likely that addition of a bulky ethyl group to the +3 and +4 phosphates is more deleterious (via steric hindrance) than simple removal of the phosphate, which imposes no steric effect. In the case of human topoisomerase I, a missing phosphate nick at +4 suppressed covalent adduct formation, whereas a nick at +3 had little effect and a nick at +1 increased the yield of covalent adduct (by permitting dissociation of the noncovalently held cleavage product) (*30*). From the results of Pourquier et al. (*30*), it appears that the human enzyme has a more stringent requirement for the nonscissile strand +4 phosphate than does the vaccinia topoisomerase. The human topoisomerase−DNA cocrystal structure reveals multiple protein contacts to the +4 and +3 phosphates of the nonscissile strand, including an interaction of the Thr-501 side-chain hydroxyl with the +3 phosphate (*21*). A mutation of the equivalent threonine of vaccinia topoisomerase (Thr-142) to isoleucine results in thermolabile topoisomerase function in vivo and in vitro (*31*).

Loss of the +1 or +2 adenosine nucleosides on the nonscissile strand reduced the rate of transesterification by factors of 20 and 1000, respectively. Does vaccinia topoisomerase directly contact the +1 and +2 nucleoside sugars and/or bases on the nonscissile strand or is the loss of base pairing to the scissile strand responsible for the missing-nucleoside effects? Earlier studies indicated that 2-*O*-methyl substitution at the +1 and +2 nucleoside sugars on the nonscissile strand did not impair covalent adduct formation by vaccinia topoisomerase (*17*). Yet, replacement of the +2A of the nonscissile strand with G (to create a +2T:G mispair) reduced the extent of covalent adduct formation by a factor

of 100 (*3*). There is a single side-chain contact between human topoisomerase I and the +1A of nucleoside of the nonscissile strand in the covalently trapped topoisomerase−DNA cocrystal, but no reported contacts with the +2A or with the sugars (*21*).

We infer from the discussion presented above that the structural basis for the interaction of cellular and poxvirus type IB topoisomerases with the DNA phosphodiester backbone of the scissile and nonscissile strands is at least partially conserved. In interpreting the deleterious effects of various DNA target site modifications on the activity of vaccinia topoisomerase, we have made the assumption that these modifications lead to the loss or perturbation of contacts with amino acids on the topoisomerase. This is the most parsimonious view of the data. We cannot exclude the possibility that some of the DNA modifications may exert their effects indirectly. A crystal structure of the viral topoisomerase in the DNA-bound state will ultimately clarify this issue.

REFERENCES

1. Shuman, S. (1998) *Biochim. Biophys. Acta 1400*, 321−337.
2. Shuman, S., and Prescott, J. (1990) *J. Biol. Chem. 265*, 17826−17836.
3. Shuman, S. (1991) *J. Biol. Chem. 266*, 11372−11279.
4. Sekiguchi, J., and Shuman, S. (1994) *Nucleic Acids Res. 22*, 5360−5365.
5. Shuman, S., Kane, E. M., and Morham, S. G. (1989) *Proc. Natl. Acad. Sci. U.S.A. 86*, 9793−9797.
6. Morham, S. G., and Shuman, S. (1992) *J. Biol. Chem. 267*, 15984−15992.
7. Stivers, J. T., Harris, T. K., and Mildvan, A. S. (1994) *Biochemistry 36*, 5212−5222.
8. Shuman, S. (1992) *J. Biol. Chem. 267*, 8620−8627.
9. Shuman, S. (1992) *J. Biol. Chem. 267*, 16755−16758.
10. Shuman, S. (1994) *J. Biol. Chem. 269*, 32678−32684.
11. Stivers, J. T., Shuman, S., and Mildvan, A. S. (1994) *Biochemistry 33*, 327−339.
12. Petersen, B. Ø., and Shuman, S. (1997) *J. Biol. Chem. 272*, 3891−3896.
13. Cheng, C., Wang, L. K., Sekiguchi, J., and Shuman, S. (1997) *J. Biol. Chem. 272*, 8263−8269.
14. Wang, L. K., Wittschieben, J., and Shuman, S. (1997) *Biochemistry 36*, 7944−7950.
15. Wittschieben, J., and Shuman, S. (1997) *Nucleic Acids. Res. 25*, 3001−3008.
16. Klemperer, N., and Traktman, P. (1993) *J. Biol. Chem. 268*, 15887−15899.
17. Shuman, S., and Turner, J. (1993) *J. Biol. Chem. 268*, 18943−18950.
18. Sekiguchi, J., and Shuman, S. (1994) *J. Biol. Chem. 269*, 31731−31734.
19. Sekiguchi, J., and Shuman, S. (1996) *EMBO J. 15*, 3448−3457.
20. Cheng, C., Kussie, P., Pavletich, N., and Shuman, S. (1998) *Cell 92*, 841−850.
21. Redinbo, M. R., Stewart, L., Kuhn, P., Champoux, J. J., and Hol, W. G. J. (1998) *Science 279*, 1504−1513.
22. Redinbo, M. R., Champoux, J. J., and Hol, W. G. J. (1999) *Curr. Opin. Struct. Biol. 9*, 29−36.
23. Sekiguchi, J., and Shuman, S. (1995) *J. Biol. Chem. 270*, 11636−11645.
24. Sekiguchi, J., and Shuman, S. (1996) *J. Biol. Chem. 271*, 19436−19442.
25. Cheng, C., and Shuman, S. (1998) *J. Biol. Chem. 273*, 11589−11595.
26. Shuman, S., Golder, M., and Moss, B. (1988) *J. Biol. Chem. 263*, 16401−16407.
27. Hwang, Y., Burgin, A., and Bushman, F. (1999) *J. Biol. Chem. 274*, 9160−9168.
28. Henningfeld, K. A., and Hecht, S. M. (1995) *Biochemistry 34*, 6120−6129.
29. Sekiguchi, J., and Shuman, S. (1997) *Nucleic Acids. Res. 25*, 3649−3656.
30. Pourquier, P., Pilon, A. A., Kohlhagen, G., Mazumder, A., Sharma, A., and Pommier, Y. (1997) *J. Biol. Chem. 272*, 26441−26447.
31. Morham, S. G., and Shuman, S. (1990) *Genes Dev. 4*, 515−524.

BI992001D